Title

Plio-Quaternary Outer Forearc Deformation and Mass Balance of the Southern Costa Rica Convergent Margin

Journal

Journal of Geophysical Research: Solid Earth, 124(9)

ISSN

2169-9313

Authors

Morell, Kristin D
Fisher, Donald M
Bangs, Nathan

Publication Date

2019-09-01

DOI

10.1029/2019jb017986

Peer reviewed

Plio-Quaternary outer forearc deformation and mass balance of the southern Costa Rica convergent margin

Kristin D. Morell[1], Donald M. Fisher[2], Nathan Bangs[3]

[1]University of California, Santa Barbara, Department of Earth Sciences, Santa Barbara, CA, United States
[2]Penn State University, Department of Geosciences, University Park, PA, United States
[3]University of Texas, Austin, Institute for Geophysics, PRC 196, 10100 Burnet Rd., Austin, TX, United States

Key Points:

- Trench retreat in southern Costa Rica can be explained by inner forearc shortening
- Outer forearc vertical deformation occurs primarily due to the subduction of bathymetric relief
- We present a new model for Plio-Quaternary deformation that does not require significant upper plate mass loss

Corresponding author: Kristin Morell, kmorell@ucsb.edu

Abstract

Identifying the processes that control the rates, magnitudes, and longevity of outer forearc deformation is fundamental to our understanding of how mass is distributed within subduction zone systems. The margin of southern Costa Rica has been the target of numerous onland field studies, geophysical surveys, and the Costa Rica Seismogenesis Project (CRISP) drilling expedition. Despite these extensive datasets, the relative roles that subduction erosion, shortening, and seamount subduction play in shaping the behavior and evolution of the outer forearc remain debated. Here we analyze new and existing geomorphic, geologic, stratigraphic, and geochronologic datasets across the entire forearc-arc-backarc system near the CRISP transect to test several conceptual models for outer forearc deformation in southern Costa Rica. The results from the compilation agree with a model where recent arcward retreat of the trench (movement of the trench in the direction of the arc) occurs due to underthrusting of the outer forearc beneath the inner forearc, and outer forearc deformation occurs primarily by transient rapid vertical tectonism due to the subduction of bathymetric relief. These results lead to a new conceptual model for Plio-Quaternary outer forearc deformation in southern Costa Rica that does not require large amounts of net mass loss within the upper plate.

1 Introduction

The rates and spatiotemporal distribution of deformation within the outer forearc of subduction zones have provided important insights into processes fundamental to how mass is distributed within subduction zone systems (e.g. von Huene & Scholl, 1991; Ranero & von Huene, 2000; Dominguez et al., 2000; Laursen et al., 2002; von Huene & Ranero, 2003; Clift et al., 2003; Allmendinger et al., 2009). Over the last 3 decades, the forearc of the nonaccretionary convergent margin at Costa Rica (Figure 1) has served as the focus of numerous investigations to understand the role of subducting bathymetry and a thinly sedimented plate on forearc evolution, including the Costa Rica Seismogenesis Project (CRISP) drilling expeditions (Vannucchi et al., 2011; Harris et al., 2013), onland field studies (Corrigan et al., 1990; Marshall & Anderson, 1995; Gardner et al., 1992; Fisher et al., 1998; Vannucchi et al., 2001; Fisher et al., 2004; Denyer et al., 2006; D. Buchs et al., 2009; D. M. Buchs et al., 2010; Morell et al., 2011; Gardner et al., 2013), and geophysical surveys (McIntosh et al., 1993; von Huene et al., 1995; Moore & Sender, 1995; Hinz, 1996; von Huene et al., 2000; Ranero & von Huene, 2000; Morell et al., 2011; Bangs et al., 2016; Edwards et al., 2018). Despite the voluminous datasets on outer forearc structure, subsidence history, and a record of slope sedimentation, there is not agreement on the processes that have shaped the Costa Rican outer forearc throughout the Plio-Quaternary, such as the relative roles of basal erosion (e.g. von Huene et al., 2004; Vannucchi et al., 2013; Vannucchi, Morgan, Silver, & Kluesner, 2016; Vannucchi, Morgan, & Balestrieri, 2016), shortening (e.g. Taylor et al., 2005), and surface exhumation (e.g. Edwards et al., 2018).

The outer forearc of southern Costa Rica, which we define as the region ∼100 km arcward from the trench (Figure 1), has undergone both subsidence and uplift at varying temporal and spatial scales since the Plio-Quaternary. This record of vertical tectonism is recorded onshore by the stratigraphy of marine sediments (e.g. Sak et al., 2004) and offshore by benthic foraminifera (e.g. Vannucchi et al., 2013), slope unconformities (e.g. Edwards et al., 2018), and seismic stratigraphy (e.g. Vannucchi, Morgan, Silver, & Kluesner, 2016). In this same region, the Middle America Trench shows evidence for upwards of 50 kilometers of retreat, or an arcward shift in the position of the trench, where the ∼200-km wide aseismic Cocos Ridge impinges on the margin (Figure 1). Both trench retreat and subsidence in this region have been related to basal erosion, or removal of the under side of the upper plate along the plate interface (Vannucchi et al., 2013). However, recent results from the CRISP drilling and seismic program (Figure 1) show that the position of the slope break has not migrated relative to the forearc since the early

Pleistocene (Edwards et al., 2018), a potential argument against basal erosion. And, it remains debated whether outer forearc subsidence is related to either basal erosion (Vannucchi et al., 2013), or slope steepening by seamount subduction (Edwards et al., 2018).

To reconcile these contrasting hypotheses, we explore several possible conceptual models for outer forearc deformation in southern Costa Rica using both onshore and offshore datasets. First, we analyze the spatial distribution of inner forearc shortening using new and previously published analyses (e.g. Fisher et al., 2004; Morell et al., 2013), and compare these results to estimates of trench retreat (e.g. Vannucchi et al., 2013). We use these datasets to test the idea that trench retreat can occur due to underthrusting of the outer forearc beneath the inner forearc (Fisher et al., 2004), a mechanism that allows for trench retreat while maintaining the relative position of the slope break. Then, we synthesize vertical tectonism records across the entire upper plate along the CRISP transect, including offshore 3D seismic and drill core (e.g. Vannucchi et al., 2011; Harris et al., 2013) and the onshore stratigraphy of marine sediments (e.g. Sak et al., 2004; Fisher et al., 2004). We use these data to compute time-averaged and incremental uplift and subsidence rates to consider several possible mechanisms for outer forearc vertical deformation, including basal erosion (e.g. Vannucchi et al., 2013; Vannucchi, Morgan, Silver, & Kluesner, 2016), shortening or extension (e.g. Edwards et al., 2018), and movement up and over roughness elements on the subducting plate (e.g. Sak et al., 2004; Edwards et al., 2018). The results from this analysis agree with a model where relative arcward retreat of the trench occurs due to underthrusting of the offshore outer forearc beneath the onshore inner forearc and arc, and outer forearc vertical tectonism occurs in rapid pulses due to the subduction of bathymetric relief.

2 Tectonic Framework and Subducting Bathymetry

In southern Costa Rica, the Cocos plate subducts northeastward beneath the Caribbean plate (locally the Panama Microplate) at the Middle American Trench at a rate of ∼80-90 mm/yr (Figure 1) (DeMets, 2001; Argus et al., 2011; Kobayashi et al., 2014). The southeasternmost portion of the Cocos plate was created by the Cocos-Nazca spreading center (Figure 1, CNS), and contains many roughness elements and bathymetric features related to overprinting by the Galápagos Hot Spot (Figure 1, GHS)(Lonsdale & Klitgord, 1978; Barckhausen et al., 2001; Hoernle et al., 2002). The most prominent of these features is the Cocos Ridge, an aseismic ridge that is >200 km wide, and exhibits a crustal thickness that approaches >20 km along its central axis (Sallarès et al., 1999; Walther, 2003). Bathymetry is highest at the crest of the Cocos Ridge (less than 1,000 m below sea level), and decreases along strike together with the crustal thickness of the Cocos plate. To the northwest of the Cocos Ridge, the Cocos plate contains numerous conical seamounts and other bathymetric features such as the Quepos Plateau, in a region that is often referred to as the seamount domain (Figure 1, SMD)(von Huene et al., 1995). In northern Costa Rica, the crust of the Cocos Plate was created by the East Pacific Rise (Figure 1, EPR). By comparison to the crust to the southeast, the morphology of the seafloor crust created by the East Pacific Rise is much smoother than the 'rough' crust to the southeast created by the Cocos-Nazca spreading center and the Galápagos Hot Spot.

The N-S-striking Panama Fracture Zone separates the Cocos plate in the northwest from the Nazca plate to the southeast near the Costa Rica-Panama border (Figure 1, PFZ). By comparison to the Cocos plate, the Nazca plate subducts at a much slower rate (∼40 mm/yr), and at a much more oblique angle (Figure 1) (Argus et al., 2011; Kobayashi et al., 2014). The bathymetry of the seafloor changes abruptly from west to east across the Panama Fracture Zone (by ∼2 km), where it truncates the Cocos Ridge on its easternmost extent. The intersection of the Panama Fracture Zone with the Middle America Trench represents the Panama Triple Junction between the Cocos, Nazca and Caribbean plates (Figure 1, PTJ). In order for the triple junction to remain stable in this tectonic

configuration (e.g. McKenzie & Morgan, 1969), it must migrate to the southeast relative to the upper plate at a rate of approximately ∼30-40 km/Ma, depending on the plate motion model (McIntosh et al., 1993; Kobayashi et al., 2014; Morell, 2015).

3 Summary of previous work on Plio-Quaternary forearc deformation Offshore

The Costa Rica Seismogenesis Project (CRISP), which includes data from IODP drilling expeditions 334 (Vannucchi et al., 2011)/344 (Harris et al., 2013) and a 3D seismic volume (Bangs et al., 2015, 2016), provides a detailed record of Quaternary vertical tectonism, deformation, and sedimentation. The study area of the CRISP program is located within the offshore outer forearc, ∼60 km to the northwest of the axis of the Cocos Ridge (Figure 1).

3.1 Incoming plate, trench, and accretionary prism

Seismic images and IODP drilling (holes U1381 and U1414) show that the incoming Cocos plate within the CRISP study area contains a relatively thin (∼100-400 m) sequence of pelagic and hemipelagic sediment sitting atop oceanic basement (Figures 2 and 3). The upper ∼50 m of this sediment section exhibits evidence for terrigenous input in the form of lithic fragments and thin sand layers (Harris et al., 2013). The toe of the upper plate contains a small accretionary prism (<10 km wide) comprised chiefly of accreted sediments imbricated by a series of landward-dipping thrusts (Figure 2) (Harris et al., 2013; Bangs et al., 2016). Approximately half of the sediments on the downgoing plate have accreted and deformed in the frontal prism while the other half has subducted below the décollement (Bangs et al., 2016). A thin (up to ∼1.5-2.0 km thick) slope cover sequence lies atop the frontal accretionary wedge, containing sediments from the shelf and slope (Harris et al., 2013; Bangs et al., 2016).

3.2 Margin wedge

Approximately >5 km landward from the toe, the margin wedge contains laterally extensive (> 30 km) layered sequences that are interpreted to represent clastic sediments (Figure 2) (Bangs et al., 2016). These sedimentary layers are extensively shortened by thrust faulting, folding and imbricate stacking and exhibit a seaward decrease in fold wavelengths (Bangs et al., 2016). There are no obvious breaks in folding and thrusting throughout the margin wedge, indicating that thrusting was a continuous process and occurred coeval with deposition of the youngest sedimentary sequences dated by drilling to be late Pliocene to early Pleistocene in age (Bangs et al., 2016; Vannucchi et al., 2011).

There are competing models about the origin and history of the margin wedge at the location of the 3D seismic volume. Vannucchi, Morgan, Silver, & Kluesner (2016) suggest that basal erosion has caused km-scale subsidence, removal of basement, and replacement of the entire margin wedge by forearc-derived sediments. However, Bangs et al. (2016) point out that the patterns of thrusting and folding visible within the margin wedge are similar to wedges in settings undergoing frontal accretion (e.g. Taiwan; Lester et al., 2013), and the overall seaward decrease in the amount of thrust displacement is consistent with this model (Davis et al., 1983).

3.3 Regional unconformity (U1)

A prominent unconformity (U1, Figures 2A & 2B), dating to the early Pleistocene (2.5 Ma), separates the margin wedge from an overlying ∼1-1.5 km thick slope cover sequence extending across most of the 3D volume (Figure 2) (Vannucchi et al., 2011; Bangs et al., 2016; Edwards et al., 2018). Evidence for shallowing water depths, subaerial ero-

sion and fluvial downcutting suggests that this regional unconformity was formed due to a late Pliocene to early Pleistocene period of rapid outer forearc uplift and subaerial exposure. Drilling at site U1379 shows that sediments below the unconformity are associated with middle abyssal paleodepths of ∼800 m, whereas sediments above the unconformity were deposited in a near-shore beach environment at paleodepths < 200 m (Vannucchi et al., 2013). Seismic imaging shows two major high-relief (∼500 m) channel systems at the unconformity surface that likely were produced by fluvial downcutting in a terrestrial environment (Edwards et al., 2018). Drilling on the middle slope at U1380 encountered a major unconformity interpreted to be U1, but paleomagnetic age constraints from this drill hole yielded a younger age for this feature of <1.3 Ma (Vannucchi et al., 2011; Harris et al., 2013).

3.4 Slope cover sequence

3.4.1 Stratigraphy and vertical tectonics

Overall, the stratigraphy of the slope cover sequence reflects progressive shallowing from the late Pliocene to the present, interrupted by several periods of short-lived uplift and subsidence. Seismic data and drilling at site U1413 indicate an accumulation of ∼1.3-1.6 km of >1.78 Ma clastic sediment at the base of the slope sediment sequence with stacking patterns as expected for sequence stratigraphy models (Harris et al., 2013; Edwards et al., 2018). These observations, together with paleodepth results from drill hole U1379, and backstripping calculations (Figure 2C), suggest rapid and widespread subsidence of ∼1200 m in the early Pleistocene (2.2 to 1.9 Ma) (Vannucchi et al., 2013; Edwards et al., 2018). This early Pleistocene subsidence is disputed to be related to either basal erosion (Vannucchi et al., 2013) or passage of the upper plate over the bathymetry across the Panama Fracture Zone (Edwards et al., 2018).

A second extensive unconformity (U2 in Figure 2), approximately ∼1.5 km above the base of the slope sediment sequence, records another pulse of uplift at 1.95-1.78 Ma (U1413; Vannucchi et al., 2011; Harris et al., 2013). Pervasive channelization and steep downcutting visible across the unconformity surface suggest it was caused by a major slope collapse in a submarine environment, potentially as a consequence of oversteepening of the slope due to seamount subduction (Edwards et al., 2018). The ∼450- 1,000 m thick clastic sediments above this unconformity exhibit sediment facies and clinoform sequences indicative of progressive shallowing, from a submarine fan complex at the bottom of the section, to an infilling slope basin near the top (Harris et al., 2013; Vannucchi et al., 2013; Edwards et al., 2018). The third and youngest major unconformity (U3 in Figure 2) within the slope sequence contains an extensive paleocanyon system, locally as much as 350 m deep, that Edwards et al. (2018) interpret to be a consequence of uplift and subaerial erosion associated with the subduction of the Quepos guyot at 1.78-1.19 Ma. The <∼200 m thick sedimentary layers above this unconformity record progressive basin infilling from ∼1 Ma to present. Vannucchi, Morgan, Silver, & Kluesner (2016) suggest that the rapid rate of sediment accumulation recorded within the uppermost slope sequence (1035 m/Ma) is a consequence of subsidence that allows terrestrial sediments to accumulate in a basin without reaching the trench.

3.4.2 Thrust and Normal Faulting

The slope cover sequence is deformed within the 3D volume, primarily exhibiting evidence for contractional deformation in the form of thrust faulting and associated folding (Figure 2) (Bangs et al., 2016; Edwards et al., 2018). Normal faults are present, but exhibit minor amounts of offset and do not cut through the entire sequence (Bangs et al., 2016; Edwards et al., 2018). The slope cover sequence exhibits a near-vertical transition, positioned close to the current shelf break (see Figure 2), between a landward region with relatively little contractional deformation and a seaward region (∼50 km land-

ward from the toe) that is more extensively folded and faulted (Edwards et al., 2018). This transition occurs at approximately the same location throughout the entire thickness of the slope cover sequence, suggesting that the wedge has maintained the same relative position since at least the early Pleistocene (Edwards et al., 2018).

4 Summary of previous work on Plio-Quaternary forearc deformation Onshore

4.1 Outer forearc

The record of Quaternary vertical tectonism on the Osa Peninsula, which is situated directly inboard of the axis of the incoming Cocos Ridge and only ∼100 km to the east of the CRISP study area (Figure 3, OP), displays many similar characteristics to the record of tectonism inferred from drilling and offshore seismic stratigraphy. The Quaternary marine section that blankets the forearc basement suggests Osa has undergone spatial and temporal periods of both rapid subsidence and uplift (Gardner et al., 1992; Sak et al., 2004; Gardner et al., 2013). Superimposed on water depth variations related to sea level fluctuations are periods of rapid (>2 m/kyr) subsidence and uplift related to trench-parallel and trench-perpendicular vertical faults that allow variable motion of distinct small (5-10 km) blocks (Sak et al., 2004; Gardner et al., 2013). This style of deformation is interpreted to result from the upper plate moving up and over the relatively small wavelength (tens of km) roughness along the crest of the Cocos Ridge, such as the series of graben structures on the ridge axis (Sak et al., 2004; Gardner et al., 2013), and suggests that this region has not accumulated a high amount of net shortening (Gardner et al., 2013).

4.2 Inner Forearc, Fila Costeña Thrust Belt

The Fila Costeña Thrust Belt is a thin-skinned mountain range that extends across the inner forearc for ∼200 km (Figure 3). This range was formed due to telescoping of the siliciclastic sediments of the Térraba basin (Fisher et al., 2004), an Eocene to late Miocene forearc basin that locally contains the Térraba and Curré Formations (Figures 4 and 5) (Phillips, 1983). This thrust belt contains a series of 3-5 thrust sheets that form a duplex, with imbricate thrusts that merge laterally with a roof thrust along leading branch lines (Sitchler et al., 2007). The base of thrust sheets is marked by the Eocene Brito Formation, a carbonate that serves as a useful marker bed in restoring hanging-wall and foot-wall cutoffs in palinspastic restorations (Figure 5) (e.g. Fisher et al., 2004). The Caribbean forearc basement below the Brito Formation is not deformed within the thrust belt, indicating that the décollement beneath the thrust belt roots between the forearc basement and the Térraba basin cover sequence.

The thrust belt is restricted to the portion of the margin where the over-thickened crust of the Cocos Ridge subducts. The development of the thrust belt has therefore been related to slab shallowing and increased coupling related to Cocos Ridge subduction (see Figure 3) (Fisher et al., 2004; Sitchler et al., 2007; Morell et al., 2008, 2013). The greatest shortening occurs within a structural culmination directly inboard of the Cocos Ridge axis (Sitchler et al., 2007). This structural culmination has the most thrust slices, the highest topography, and laterally extensive landslides along the trench-facing side of the topographic divide (Figure 5). The number of thrusts decreases laterally both to the northwest and southeast from this culmination. In the northwest, the thrust belt terminates near the Herradura Block, where the margin becomes influenced by seamount subduction (Figure 3, HB) (Fisher et al., 1994). In the southeast, shortening diminishes to zero near the onland projection of the Panama Fracture Zone (Sitchler et al., 2007; Morell et al., 2008, 2013). Given the migration of the Panama Fracture Zone and Panama Triple Junction to the southeast through time relative to the upper plate, it has been shown

that the thrust belt also migrates, as areas to the southeast exhibit lesser amounts of shortening with distance along strike (Morell et al., 2008, 2013).

Several lines of evidence based on geologic, stratigraphic and geomorphic data suggest the Fila Costeña Thrust Belt has been actively shortening and steadily uplifting at moderate rates throughout the Quaternary. A marine terrace located at ∼1.2 m above mean sea level (Figure 5, Qs) contains a shell with a radiocarbon age of 5.54 ± 0.07 ka, near where the Térraba River intersects the frontal thrust (Fisher et al., 2004). Quaternary fluvial terraces along the Térraba River are displaced by thrust faults (Fisher et al., 2004). And, deformed lahars within the southeastern portion of the thrust belt are radiocarbon-dated to be Quaternary in age (Morell et al., 2013).

Although these datasets indicate that the Fila Costeña must have been active throughout the Quaternary, the exact timing of initiation of thrusting is less well constrained. There are two cited age constraints relating to the onset of uplift of the Fila Costeña. The oldest relates to Miocene-aged gabbroic intrusions of the Puerto Nuevo Formation exposed with the thrust belt (Alvarado & Gans, 2012). Mescua et al. (2017) posit that these intrusions are related to the initiation of thrust faulting (Kolarsky et al., 1995), and therefore suggest that the initiation of the Fila Costeña thrusting began in the Miocene. The second constraint comes from the presence of a deformed Pliocene marine mudstone that caps the sedimentary units of the Térraba basin and unconformably underlies the Pliocene Paso Real Formation (Kesel, 1983; Sitchler et al., 2007). This mudstone has been used by several authors (Fisher et al., 2004; Sitchler et al., 2007) as a maximum constraint on the timing of the initiation of shortening and uplift within the Fila Costeña, because it indicates submarine conditions leading up until Pliocene time. Mescua et al. (2017), in contrast, suggest that the unconformity at the base of this mudstone could be related to a Miocene deformation event.

4.3 Volcanic Arc

The décollement of the Fila Costeña is hypothesized to extend downdip to root beneath the uplifted Cordillera de Talamanca volcanic arc to form an orogen-scale pop-up structure together with back thrusts in the Limón back arc basin (Figures 3 and 4) (Fisher et al., 2004; Brandes et al., 2007; Morell et al., 2012; Morell, 2016). Evidence for uplift of the Talamanca compared to adjacent arc segments has long been suggested because of their anomalously high elevations (de Boer et al., 1995; Gräfe et al., 2002). Late Miocene extinction of calc-alkaline volcanism within this range had been associated with uplift of the Talamanca due to Cocos Ridge subduction (de Boer et al., 1995; Abratis & Wörner, 2001). However, similar-aged extinction of adjacent arc segments in Panama (Wegner et al., 2010) suggest that late Miocene shut-off of calc-alkaline active volcanism in the Talamanca was not linked to Cocos Ridge subduction and was rather related to a late Miocene plate tectonic reconfiguration (Morell et al., 2012; Morell, 2015; Rooney et al., 2015). The increase in range width, high elevations, and deeply incised river reaches draining the Talamanca suggest ongoing and recent rock uplift within the past few million years (Morell et al., 2012). A surface with significantly lower relief and gentler stream gradients located at elevations above ∼2000-2500 m near the range peaks suggests the Talamanca underwent significantly lower rock uplift rates at a time period no earlier than ∼2-3 Ma (Morell et al., 2012). This timing of uplift coincides with the timing of subduction of the Cocos Ridge as derived from plate reconstruction models, and therefore suggests that Cocos Ridge subduction and uplift of the Talamanca are linked (MacMillan et al., 2004; Morell et al., 2012). Recently, Mescua et al. (2017) argue that deformation within the Talamanca must have begun in the Miocene, due to the presence of an angular unconformity between Miocene sandstones of the Pacacua Formation beneath undeformed andesites of the Grifo Alto Formation (dated to 7.3 to 2 Ma) (Alvarado & Gans, 2012).

5 Is trench retreat linked to upper plate shortening farther inboard?

5.1 Approach and methods: analysis of new and existing data

We test the idea that a portion of the trench retreat in southern Costa Rica is related to underthrusting within the inner forearc, by comparing lateral variations in trench retreat to along-strike changes in shortening within the Fila Costeña Thrust Belt. In the absence of accretion, movement of the outer forearc under the inner forearc could lead to trench retreat without basal erosion. If so, there should be a relationship between the amount of shortening in the inner forearc at the Fila Costeña and the amount of trench retreat for a given position along strike.

In order to evaluate how shortening in the Fila Costeña varies along strike, we compiled new and existing structural data from the thrust belt, constructed one new balanced cross section, and synthesized published shortening estimates (Figure 5) (Fisher et al., 2004; Sitchler et al., 2007; Morell et al., 2013). The structural data used in this study (orientations and locations of contacts, bedding and faults) are based both on previously published data from the central and southern portions of the thrust belt (Kolarsky et al., 1995; Fisher et al., 2004; Sitchler et al., 2007; Morell et al., 2013), as well as ∼75 new structural measurements from the northwestern portion of the thrust belt. Our new cross section was constructed by forward modeling in Midland Valley's 3D Move to match mapped contacts, thrust traces and ∼20 surface structural measurements. Shortening was estimated by line-length balancing, and restoring hanging-wall to foot-wall cut offs within the Brito Formation following methods in Fisher et al. (2004). Where hanging wall cut offs were not directly observed in the field, they were placed directly above the current erosional surface to obtain a minimum fault slip estimate.

Unfortunately, estimation of shortening by line-length balanced cross sections is spatially limited within the Fila Costeña. There are few age constraints within the turbidites of the Térraba Formation, making it difficult to recognize stratigraphic position among thrusts that do not expose the Brito Formation at the surface. This situation particularly arises in the northwesternmost portion of the thrust belt, where the décollement steps up section to the northwest above the Brito Formation along a lateral ramp (Figure 5) (Fisher et al., 2004). This lack of stratigraphic control creates a problem because the line-length balancing method requires a key bed with which to match hanging wall and footwall cut-offs. Moreover, there are some regions of the thrust belt where structural data are unattainable due to cover by younger volcanic units, thick vegetation, high rates of saprolite production, and/or poor exposure. These shortcomings make it difficult to compare shortening between positions along-strike.

To evaluate relative along-strike changes in shortening across the entire thrust belt, including those regions where line-length balanced shortening estimates are not possible, or where cover or vegetation introduces large uncertainties in the structure, we calculated the total cross-sectional area of the Fila Costeña relative to current sea level within 10 km-wide- and 30-km-long swaths (Figure 6), and compared these estimates to the elevation of the divide of the range. We use topography and cross-sectional area as a proxy for shortening with the thrust belt on the basis that simple orogenic wedge models predict that the addition of material at the toe of a wedge will lead to increases in the width and height of the wedge (i.e. a conservation of mass for a wedge-shaped geometry) (e.g. Davis et al., 1983).

Finally, we compare our estimates of forearc shortening with published trench retreat amounts as reported in Vannucchi et al. (2013). Although the previous position of the trench is not known, we follow Vannucchi et al. (2013) in measuring trench retreat as the arcward distance from the current trench to the assumed location of the trench prior to retreat (305° trend line as shown in Figures 1 and 3, dot-dashed line).

5.2 Results: Lateral variations in shortening within the Fila Costeña Thrust Belt

In the southeastern portion of the thrust belt, our results show both divide elevation and cross-sectional area decrease laterally to the southeast in tandem with shortening as measured from balanced cross sections (Figure 7). The region of the thrust belt with the most estimated shortening (∼37 km), the highest topography (∼1,600 m) and the greatest number of thrusts at cross-section D (Figures 5-7) exhibits the largest total cross-sectional area of 21 ± 4 km^2. From this position of greatest shortening, balanced cross-sections indicate that shortening decreases steadily and relatively rapidly to the southeast along strike until diminishing to only ∼4 km near where the thrust belt tips out laterally. This ∼30 km decrease in shortening over a ∼50 km distance corresponds with a ∼1,000 m drop in the elevation of the divide and a ∼8 km^2 decrease in the cross-sectional area of the thrust belt (Figure 7).

Similar lateral decreases in topography and shortening are observed in the northwestern region of the thrust belt. We estimate ∼16 km of shortening along the Térraba River from our new cross section (cross-section C, Figure 5). This estimate is ∼15 km less than shortening calculated by Sitchler et al. (2007) for this same section, a discrepancy due in large part to differing interpretation of the amount of slip required on the rearmost thrust. As most hanging wall cut-offs were placed at the erosion surface, the line-length balanced shortening estimate for our new cross-section is primarily based on: 1) the thrust fault dip, which averages between 15-35°for the entire thrust belt, and 2) the depth to décollement, estimated to be between 2500-3000 m by Sitchler et al. (2007). Based on these constraints, we estimate the total uncertainty in our line-length balanced shortening estimate to be between 10-20%. Nonetheless, shortening decreases by at least 4-15 km laterally over the ∼8 km distance between cross-sections D and C. The elevation of the divide and cross-sectional area also decline northwestward across this interval, but topography is further decreased due to steep downcutting by the Térraba River (Figures 6 and 7). To the northwest of the Térraba River, line-length-balanced shortening estimates cannot be obtained because the Brito Formation is not exposed. But, after excluding those regions where topography is strongly affected by Térraba River incision, the laterally diminishing cross-sectional area suggests that shortening decreases gradually to the northwest for >100 km along strike until the thrust belt eventually terminates (Figures 5 and 7).

Taken together, these results suggest that inner forearc shortening at the Fila Costeña Thrust Belt steadily decreases laterally away from the position of greatest shortening inboard of the Cocos Ridge axis (at cross-section D). These decreases in shortening occur relatively gradually to the northwest for ∼150 km along strike and more rapidly to the southeast for ∼50 km along strike.

5.3 Results: Lateral variations in trench retreat scale with inner forearc shortening and crustal thickness of the Cocos plate

The amounts of trench retreat in southern Costa Rica display similar along-strike patterns as shortening and topography within the Fila Costeña Thrust Belt and with the crustal thickness of the subducting Cocos plate. Trench retreat is highest (∼50 km) near cross-section D where Cocos plate crustal thickness, inner forearc shortening, cross-sectional area and divide elevations are likewise greatest (Figure 7). The magnitude of trench retreat then tapers parallel to strike in a manner similar to shortening and lower plate crustal thickness estimates. The largest lateral gradient in trench retreat occurs in the southeastern portion of the range, where shortening rapidly decreases to the southeast near the termination of the thrust belt and the downgoing plate transitions from the Cocos to Nazca plate (Figure 7). Northwest of the position of greatest shortening, trench retreat estimates gradually decrease to less than 30 km at the Herradura Block

(Figure 3, HB), where the crustal thickness of the downgoing Cocos plate diminishes to <10 km (Figure 7). Overall, these results suggest that trench retreat scales with inner forearc shortening at the Fila Costeña Thrust Belt and with the thickness of the crust of the subducting Cocos plate.

6 What causes outer forearc vertical tectonism in southern Costa Rica along the CRISP transect?

6.1 Approach and methods: analysis of existing data

We use the spatial distribution and rate of upper plate vertical tectonism to distinguish between possible mechanisms for outer forearc deformation. Using the present-day roughness of the subducting plate, and the convergence rate of 9.5 cm/yr, Sak et al. (2004) show that the average subsidence or rock uplift rate due to the subduction of km-scale bathymetric relief exceeds 2 mm/yr, with a short duration (<1 Myr) and length scale (∼5 km). We therefore hypothesize that rock uplift or subsidence caused by seamount subduction (e.g. Edwards et al., 2018) should be rapid (>1 m/kyr), short in duration (<1 Myr), spatially irregular (over distances <10 km), and with a magnitude similar to the height of the bathymetric feature. In contrast, previous authors suggest that subsidence induced by basal erosion has occurred across the 350 km strike-length of the indented portion of the margin (Figure 3), and has been occurring near-continuously since the past 2.2 Ma (e.g. Ranero et al., 2008; Vannucchi et al., 2013). We therefore hypothesize that subsidence due to basal erosion should be longer-lived (>1 Myr) and occur on larger spatial scales (>10 km) than deformation caused by seamount subduction.

To discriminate between these potential mechanisms of deformation, we compiled published data to calculate rock uplift and subsidence rates across the entire upper plate near the CRISP transect, including offshore and onshore regions. For offshore data, we used the published data to calculate incremental rock uplift or subsidence rates using the magnitudes and timing of vertical tectonics from IODP drill hole U1379 (Vannucchi et al., 2013; Vannucchi, Morgan, Silver, & Kluesner, 2016). Onshore, we used these published data to compute uplift and subsidence rates based on the elevation and depositional location of radiocarbon and optically stimulated luminescence (OSL) samples collected from Quaternary marine sediments. The published data were derived from Gardner et al. (1992), Fisher et al. (2004), Sak et al. (2004), Sak et al. (2009), and Gardner et al. (2013). In our analysis, we calibrated each radiocarbon date to calendar years using OxCal v.4.3.2 (Bronk Ramsey, 2009) (calibration curve from Reimer et al. (2013)), and calculated time-averaged rock uplift or subsidence rates for each OSL or calibrated radiocarbon sample following methods in Gardner et al. (2013). This calculation involves dividing the sample age from the difference between its modern elevation, depositional position relative to modern sea level (facies depth), and paleo sea level at time of deposition. In all uplift/subsidence rate calculations, we used the paleo sea level curve of Lambeck et al. (2014) for sample ages between 35 ka to present and the Lambeck & Chappell (2001) sea level curve for ages older than 35 ka. Using this same procedure, we calculated incremental uplift or subsidence rates where possible for each location that contained more than one age, by using the differences in both elevation and age between the two samples. Where no OSL or radiocarbon dates were available, we used relevant published geologic, geomorphic and stratigraphic data to consider the timing and duration of vertical deformation across the forearc.

6.2 Results from the outer forearc: Rapid and short-lived (<1 Myr) cycles of vertical tectonism both onshore and offshore

6.2.1 Offshore outer forearc

In the offshore forearc, cycles of rapid uplift and subsidence since the early Pleistocene have occurred over relatively short time periods (<1 Myr), with magnitudes less than ∼1 km (Table 1 and Figure 8). After backstripping to account for the effects of sediment loading (Vannucchi et al., 2013), the record at drill hole U1379 begins in the early Pleistocene with a pulse of 0.8 ±0.1 km of rock uplift at a rate of 2.7 ± 0.1 km/Myr over the 0.3 Myr time interval between 2.5 to 2.2 Ma (Table 1 and Figure 8B), which produced unconformity U1 (Figure 2). This pulse of uplift was immediately succeeded by a similarly short-lived episode of 1.2 ± 0.1 km of subsidence at a rapid rate of 5.9 ± 0.2 km/Myr over the 0.2 Myr time interval between 2.2 to 2.0 Ma (Table 1 and Figure 8). Following this ∼500-kyr cycle of rapid uplift and subsidence, the remaining record in the U1379 drill hole reveals a temporary period of slow subsidence for 100 kyr, followed by relatively slow uplift from 1.9 Ma to present (Table 1 and Figure 8). Thus, the vertical record in drill hole 1379 indicates a pulse of rapid uplift and subsidence over a ∼ 1 Myr interval in the early Pleistocene, followed by slow uplift for the remaining ∼2 Myr to the present (Figure 8B).

Unconformities and depositional environments recorded within the slope cover sequence in the 3D seismic volume show two additional Pleistocene uplift-subsidence cycles that are not recorded in hole 1379 (Figure 3): one at 1.95-1.78 Ma (U2 in Figure 2; Vannucchi et al., 2011; Harris et al., 2013) and a second at 1.78-1.19 Ma (U3 in Figure 2; Edwards et al., 2018). Why U2 and U3 are not recorded in drill hole 1379 remains unclear, but Site 1379 is offset ∼15 km from the 3D volume and the differences in age may indicate a short lateral extent of the unconformity. Rapid rates of sediment accumulation (1035 m/Ma) within the uppermost portion of the slope sequence have been used by Vannucchi, Morgan, Silver, & Kluesner (2016) to argue for recent rapid basin infilling due to subsidence by basal erosion. Nevertheless, an incremental uplift or subsidence rate cannot be calculated from these data because the exact magnitude and timing of vertical tectonism associated with these features remains underconstrained.

6.2.2 Onshore outer forearc at the Osa Peninsula

Although occurring over time periods, the cycles of rapid uplift and subsidence offshore at CRISP occur at similar rates and comparable durations as short-term (<1 Myr) vertical tectonism observed on the Osa Peninsula onshore. Thirteen ^{14}C and 4 OSL samples (Gardner et al., 1992; Sak et al., 2004; Gardner et al., 2013) collected on the Osa Peninsula span in age from ∼20-40 ka, and yield high net rates of time-averaged rock uplift, ranging from 1.9 ± 1.3 m/kyr to 8.0 ± 2.4 m/kyr (Tables 2 and 3). On the northwestern portion of the peninsula, calculated incremental rates indicate subsidence amongst disparate tectonic blocks has occurred in excess of 5 m/kyr over time spans of ∼5-8 kyr: 5.1± 1.9 m/kyr of subsidence over the interval ∼38-45 ka (Table 2, samples 142204 and 142205), 7.7± 2.3 m/kyr of subsidence over the interval ∼39-44 ka (Table 2, samples 154116 and 154117), and 8.2±1.3 m/kyr of subsidence over ∼31-39 ka (Figure 8 and Table 2, samples 154117 and 142208) (Sak et al., 2004). Thus, although the Osa Peninsula has undergone rapid net uplift since ∼40-50 ka associated with the emergence of the peninsula (Gardner et al., 1992; Sak et al., 2004; Gardner et al., 2013), the relatively small tectonic blocks on the peninsula have also undergone periods of short-lived, rapid vertical tectonism, with a style of deformation much like the ∼2.5 to 2 Ma record observed within the CRISP study area.

6.3 Results from the onshore inner forearc and arc: Long-lived vertical tectonism (>1 Myr)

The sequences of rapid Pleistocene outer forearc uplift or subsidence contrast with the duration and magnitude of vertical tectonism observed in the inner forearc at the Fila Costeña, and the volcanic arc at the Cordillera de Talamanca onshore. Records of deformation in each of these regions suggest they have experienced moderate and steady rates of uplift (>0.5 m/kyr) from at least the Pliocene to present.

6.3.1 Inner forearc at the Fila Costeña Thrust Belt

Near where the Térraba River intersects the frontal thrust of the Fila Costeña, a shell from the marine terrace located at ∼1.2 m above mean sea level (Figure 5, Qs) yields a Holocene uplift rate on the order of 0.5±0.4 m/kyr (Fisher et al., 2004) (Table 2 and Figure 8). Assuming that incision has kept apace with rock uplift, fluvial terraces along the Térraba River located ∼90 m above current base level suggest that rock uplift has persisted continuously over hundreds of thousands to millions of years, since at least MIS 5 or 7 (∼200 kyr) (Fisher et al., 2004). Thrust displacement of these fluvial terraces, and back-tilted late Pleistocene lahars along cross section G (Figure 5) (Sitchler et al., 2007; Morell et al., 2013), further indicate that deformation in the Fila Costeña must have been ongoing throughout the Quaternary or longer.

6.3.2 Cordillera de Talamanca volcanic arc

Geomorphic and topographic evidence suggests that the Cordillera de Talamanca volcanic arc has likewise been steadily uplifting for the past ∼1-3 Ma. On the northeastern flanks of the range, a low-relief surface at elevations >∼2 km that contrasts with steep downstream channel segments is proposed to reflect a recent pulse of rock uplift and increased incision that began no earlier than ∼2-3 Ma (Morell et al., 2012). Assuming that uplift is equally balanced by erosion, the elevation of 21 knickpoints along the edge of the low relief surface relative to current base level yields an average of 1.8 ± 0.3 km of rock uplift since the onset of increased incision (see Figure 3 and Morell et al., 2012). The role of precipitation or substrate erodibility is ruled out as a large factor in the development of these knickpoints, because the knickpoints do not coincide with changes in lithology, and there are not observed gradients in rainfall throughout the study area (Morell et al., 2012).

Assuming that fluvial erosion rates within the Talamanca are comparable to rates in similar tectonically active settings such as Tibet (e.g. Ouimet et al., 2009) or adjacent Panama, the erosion rates within this region of the Talamanca likely approach ∼0.3-0.5 mm/yr (Gonzalez et al., 2016). Given that the knickpoints and low-relief surface are still preserved within this transient landscape, such relatively fast erosion rates imply that the initiation of the increased incision and rock uplift of the Talamanca as recorded by the knickpoints must have occurred at a time period less than 1-3 Ma (Morell et al., 2012). Using 1-3 Ma as the initiation of uplift, the Talamanca have been uplifting at a mean rate of 0.6 ± 0.1 to 1.8 ± 0.3 m/kyr (Figure 8). The rock uplift rates for the Talamanca are therefore within the same order of magnitude (>0.5 m/kyr) and similar duration (>1 Myr) as those estimated for the Fila Costeña Thrust Belt.

7 Discussion

Based on the analysis, we argue for the conceptual model depicted in Figure 9 for Plio-Quaternary deformation in southern Costa Rica. In this model, trench retreat occurs due to underthrusting associated with long-term (>1 Myr) shortening within the inner forearc-arc-backarc as a consequence of Cocos Ridge subduction. These long-term processes contrast with rapid, short-term (<1 Myr) pulses of outer forearc vertical tec-

tonism both onshore at the Osa Peninsula and offshore at CRISP, processes which we suggest occur due to the subduction of seamounts or other short-wavelength bathymetric relief.

7.1 Trench retreat in the outer forearc related to Plio-Quaternary upper plate shortening and crustal thickening

From a mass balance perspective, the observed correlations between trench retreat and inner forearc shortening support the idea that a significant portion of the measured trench retreat could be caused by underthrusting beneath the inner forearc (Figure 9). Where trench retreat is highest (Figure 7), line-length balanced cross sections indicate that shortening in the Fila Costeña could account for as much as 40% of the total measured trench retreat. However, shortening within the Fila Costeña must be higher than the estimates reported from balanced cross sections, because most hanging wall cut-offs are now eroded, and thus the shortening amounts plotted in Figure 7C represent minimum estimates. Moreover, these shortening estimates do not account for any crustal thickening related to the currently uplifting Cordillera de Talamanca volcanic arc farther landward (Gräfe et al., 2002; Morell et al., 2012), or to documented shortening in the back arc along the Limón back arc thrust belt (Figures 3 and 9; Brandes et al., 2007). Thus, the total amount of trench retreat related to underthrusting and upper plate crustal thickening could be much higher than the shortening calculated by line-length balancing within the Fila Costeña alone.

Crustal thickening and long-term uplift in the upper plate at moderate rates (0.5-1 mm/yr of uplift; Tables 2 and 3) are supported by numerous lines of evidence, including elevated marine and fluvial terraces in the Fila Costeña and the elevation of knickpoints high within the Talamanca Range (Figure 3). If this crustal thickening occurs together with underthrusting of the outer forearc, as we propose, net subsidence should be occurring in the footwall of the frontal thrust of the Fila Costeña offshore, due to flexural loading (Figure 9). This idea is supported by inferences by Vannucchi, Morgan, Silver, & Kluesner (2016), who use the relatively rapid rate of sediment accumulation (1035 m/Ma) within the upper slope sequence as evidence that sufficient subsidence has created accommodation space to allow terrestrial sediments to accumulate within a forearc basin without reaching the trench. Although Vannucchi, Morgan, Silver, & Kluesner (2016) argue that this subsidence has occurred due to mechanical erosion at the base of the margin wedge, our proposed model for displacement of the outer forearc beneath the Fila Costeña predicts that long-term subsidence should be occurring at this portion of the margin, without the need for basal erosion. Unfortunately, direct observation of subsidence is currently not possible because there are no published datasets in the offshore area within the footwall of the frontal thrust of the Fila Costeña (See Figures 8 and 9). Thus, although there is abundant evidence for uplift and crustal thickening in the upper plate onshore, the question of whether net subsidence has occurred in this offshore region and the potential subsidence mechanisms remain unresolved.

Plio-Quaternary underthrusting beneath the inner forearc and arc helps explain why the shelf break has remained in the same position relative to the trench since the Pliocene (Edwards et al., 2018), despite evidence for trench retreat during this same time period. The Holocene marine terraces and displacement of Quaternary deposits, and the presence of a Pliocene or younger low-relief surface at high elevations (Figure 3) confirm that crustal thickening within the forearc and arc occurred during the same Pliocene to Recent time period when forearc drilling and seismic records suggest that the shelf break has remained stationary relative to the forearc (Edwards et al., 2018). However, Mescua et al. (2017) argue that deformation in the Fila Costeña and the Talamanca began in the Miocene, a potential argument against Plio-Quaternary deformation in the upper plate. Mescua et al. (2017) posit that Miocene intrusions within the Fila Costeña Thrust Belt are related to the initiation of faulting (Kolarsky et al., 1995), but detailed

mapping of the thrust belt (Fisher et al., 2004; Sitchler et al., 2007; Morell et al., 2008, 2013) indicates that these intrusions do not cross-cut thrust faults, and therefore may be older than the faulting.

Mescua et al. (2017) further argue that deformation within the Talamanca must date to the Miocene, due to the presence of an angular unconformity between Miocene sandstones of the Pacacua formation beneath undeformed andesites of the Grifo Alto formation (dated to 7.3 to 2 Ma) (Alvarado & Gans, 2012), but the presence of this angular unconformity does not preclude Plio-Quaternary uplift. Exhumation and uplift of the Talamanca are proposed to occur by a pop-up structure (Figure 4) (Fisher et al., 2004; Morell et al., 2012), along faults in the inner forearc and backarc (Brandes et al., 2007), and uplift along such a structure (Morell et al., 2012) does not require tilting. Regardless of the initial timing of deformation in this region, the deformation of Quaternary deposits (Sitchler et al., 2007; Morell et al., 2013) and rapid recent incision in the Talamanca (Morell et al., 2012) indicate that the upper plate of southern Costa Rica must have been accumulating shortening since at least the Pliocene to present, during the same time period when the shelf break maintained its relative position offshore (Edwards et al., 2018).

7.2 Plio-Quaternary trench retreat and upper plate crustal thickening related to Cocos Ridge subduction

The spatial correlations between the thickness of the subducting Cocos plate crust and the total amounts of trench retreat and inner forearc shortening (Figure 7) suggest that Plio-Quaternary trench retreat and upper plate crustal thickening are related to the late Pliocene to Recent subduction of the Cocos Ridge. The greatest amounts of trench retreat and inner forearc shortening occur where the subducting Cocos plate thickness approaches 20 km at the ridge axis (Figure 7). From this point of greatest crustal thickness, both trench retreat and inner forearc shortening decrease along strike similarly to the thickness of the subducting Cocos plate crust (Figure 7). The observation that the length of the Talamanca, Fila Costeña, and Limón back arc thrust belt are restricted to the areas experiencing Cocos Ridge subduction further agrees with this hypothesis (Figure 5). These relationships suggest that shortening in the Fila Costeña could be related to slab shallowing due to a buoyant and over-thickened Cocos Ridge, following conclusions from many previous studies (e.g. Sitchler et al., 2007; Morell et al., 2008, 2013). Although recent geophysical images show that the slab beneath the Talamanca Range may contain a steeply-dipping leading edge (Dzierma et al., 2011), the location of the geophysical transect lies several tens of kilometers to the northwest of the Cocos Ridge axis. Thus, the dip of the slab along the geophysical transect may not be representative of the slab geometry along the Cocos Ridge axis (Morell, 2015).

7.3 Frontal erosion, basal erosion, or underplating inboard of the seamount domain

Figure 7 shows upwards of ∼20 km of trench retreat inboard of the subducting seamount domain, beyond the northwestern extent of the Fila Costeña Thrust Belt and where no extensive amounts of forearc shortening have been calculated. Exactly what causes trench retreat in this seamount domain region remains underconstrained, but possible explanations include basal or frontal erosion (e.g. Ranero & von Huene, 2000) and/or crustal thickening and shortening due to seamount subduction. Evidence for frontal erosion, or removal of upper plate material by offscraping near the toe, is documented by high-resolution bathymetric images of the trench and outermost forearc (Ranero & von Huene, 2000). These images show local trench retreat in the form of scalloping and scarring of the outer slope directly inboard of subducting seamounts (Figure 3) (von Huene & Scholl, 1991; Ranero & von Huene, 2000). Evidence for deformation by seamount subduction is supported by styles of deformation within the inner forearc inboard of the seamount domain.

Here, several tectonic blocks bound by margin-perpendicular faults display lateral wavelengths that are similar to the size of subducting bathymetric features (Figure 3) (Fisher et al., 1998, 2004; Sak et al., 2009). Trench retreat could result if this deformation by seamount subduction is also associated with crustal thickening and shortening (Fisher et al., 1998; Sak et al., 2009).

7.4 Pleistocene to Recent pulses of outer forearc rapid vertical tectonism related to subducting bathymetric features

Unlike the long-term uplift, shortening and crustal thickening in onshore regions, the late Pliocene to Recent offshore record from the CRISP study area displays rapid cycles of deformation that occur over time scales less than 1 Myr. We suggest that these rapid cycles of uplift and subsidence were caused by slope steepening due to the subduction of ∼1 km-high roughness elements on the Cocos plate (Edwards et al., 2018), in a manner similar to deformation on the Osa Peninsula (Sak et al., 2004). We make these conclusions based on several lines of reasoning.

First, the total magnitudes of the rapid uplift and subsidence cycles within the 3D volume are comparable to the height of bathymetric relief currently on the Cocos plate seaward of the deformation front. The results in Table 1 and in Figure 2C, based on backstripping the sediment column at IODP site 334-U1379 (Vannucchi et al., 2013), show that the magnitude of the uplift/subsidence cycle recorded at this drill hole ranges from ∼0.8-1.2 km over the time period of ∼2.5-2 Ma. As shown in Figure 7D, the Quepos plateau is the tallest of the features offshore currently, and this feature is similarly approximately ∼1 km in height.

Second, as shown in Table 1 and Figure 8B, the entire uplift and subsidence cycle recorded by U1379 does not exceed ∼ 0.5 Myr in duration and is associated with relatively rapid incremental vertical tectonism rates (∼3 mm/yr in uplift and ∼6 mm/yr of subsidence). As shown by Sak et al. (2004), vertical tectonism at such a high rate and over such a short time period is an expected result if deformation occurs by seamount subduction given a roughness element of ∼1 km, and a convergence rate of 80-90 mm/yr. The 3D volume shows relatively minor amounts of continuous thrusting and folding (∼15-20%) throughout the Plio-Quaternary, and these faults and folds are unlikely to be solely responsible for such rapid vertical deformation (Bangs et al., 2016; Edwards et al., 2018).

Third, the magnitude and short duration of the uplift-subsidence pulses observed within the CRISP transect are highly similar to deformation styles observed onshore at the Osa Peninsula (e.g. Sak et al., 2004). On Osa, the OSL and radiocarbon ages from marine sequence yield average incremental subsidence/uplift rates on the order of >5 mm/yr over periods of 5-8 kyr (Table 2 and Figure 8). These transient rapid uplift or subsidence rates have been demonstrated to occur by simple shear on subvertical faults that adjust to changes in the slope and height of subducting relief, without large amounts of shortening or extension (Sak et al., 2004; Gardner et al., 2013). The fact that the Quaternary vertical tectonism recorded both onshore at the Osa Peninsula and offshore at CRISP occurs over similar rates and for comparable durations but is separated by less than 100 km distance, suggests that they likely occur due to a similar mechanism.

Finally, plate reconstruction models independently indicate that the CRISP outer forearc region has experienced the subduction of high-relief bathymetric features such as fracture zones, seamounts and plateaux during the same time periods that the prominent unconformities (Figure 2) were forming within the CRISP study area. The first major early Pleistocene unconformity (U1) coincides with a time when reconstructions suggest that the CRISP study area should have been experiencing the effects of the oblique passage of the km-scale relief associated with the Panama Fracture Zone (Morell, 2015). The additional two uplift-subsidence cycles recorded within the slope sequence (U2 and U3 at ∼1.9 Ma and ∼1.3 Ma, respectively) coincide with the time when the CRISP study

area was experiencing the subduction of Cocos plate crust with a high number of seamounts and plateaux (seamount domain) (Morell, 2015; Edwards et al., 2018).

7.5 Implications for mass balance along the Costa Rica subduction zone

The Costa Rican subduction zone has long been recognized as a type example of an erosive margin, undergoing significant amounts of basal erosion, outer forearc subsidence and trench retreat (Vannucchi et al., 2001, 2013). But, the processes we describe as illustrated on Figure 9 do not require significant amounts of upper-plate mass loss. The offshore data do not show evidence for widespread upper plate extension, as is often noted in erosive margins setting such as the Andes (Clift & Vannucchi, 2004), and we suggest that more than half of the trench retreat could be related to contraction occurring across the upper plate. The suggestion that the major unconformities in the offshore slope sequence are related to short-lived uplift and subsidence cycles due to bathymetric relief (Edwards et al., 2018) further implies that basal erosion may not be the only mechanism producing outer forearc subsidence in this region. In total, these observations imply that large amounts of basal erosion may not be required along this portion of the southern Costa Rican margin, at least since the onset of Cocos Ridge subduction in the Plio-Quaternary.

Whether accretion or erosion has dominated this margin prior to the late Pliocene subduction of the Cocos Ridge remains a matter of debate. Images of the Pliocene and older margin wedge within the 3D volume below the slope sequence show laterally extensive layered sequences that have been interpreted as clastic bedding (Vannucchi, Morgan, Silver, & Kluesner, 2016; Bangs et al., 2016). The occurrence of layered clastic sequences in the margin wedge could be explained by a scenario where sediment was originally deposited on the subducting plate and subsequently frontally accreted, shortened and thickened (Bangs et al., 2016). The presence of clastic sediments, thrust faulting and imbricate stacking, as seen in the CRISP 3D volume (Bangs et al., 2016; Edwards et al., 2018), are observations consistent with a frontal accretionary model, common in many global margin wedges (e.g. Lester et al., 2013). At the time of accumulation of the sediments within the margin wedge (> 2.2 Ma) (Vannucchi et al., 2011), the region of the CRISP transect was experiencing the effects of relatively slow and oblique Nazca subduction (Morell, 2015). This tectonic setting was likely more favorable to frontal accretion (Bangs et al., 2016), given analogous conditions along the western Panamanian margin, where seismic reflection profiles show an active accretionary wedge is actively developing immediately to the east of the Panama Fracture Zone inboard of Nazca plate subduction (MacKay & Moore, 1990; Moore & Sender, 1995) (Figure 1).

8 Conclusions

Using compiled geologic, geomorphic, stratigraphic and geochronologic data across the entire upper plate, we present a new model for Plio-Quaternary outer forearc deformation of southern Costa Rica. In this model, trench retreat is a natural consequence of wholesale movement of the outer forearc beneath the inner forearc due to shortening, uplift and contraction across the terrestrial portion of the upper plate due to Cocos Ridge subduction. And, outer forearc deformation both terrestrial and submarine, is dominated by short pulses of uplift and subsidence related to the subduction of bathymetric features, with only minor amounts of internal shortening or extension. Although the subducting Cocos plate in this region of southern Costa Rica is thinly sedimented, and the toe of the margin exhibits minor amounts of accretion, the processes we describe do not require significant amounts of upper-plate mass loss inferred at the base of the forearc along thinly sedimented margins.

Acknowledgments

All data are listed in the tables, supporting information, and references within the text. This work was primarily funded by the Tectonics program of the National Science Foundation via grants EAR-9909699 (DF), EAR-0738941 (DF), and EAR-1756943 (KM). All the drilling-related data are publicly available at www.iodp.org. We are grateful for comments on this manuscript by two anonymous reviewers, and the associate editor. We thank D. Oakley for help with construction of Figure 5. Move software was generously provided by Midland Valley under their Academic Software Initiative.

References

Abratis, M., & Wörner, G. (2001). Ridge collision, slab-window formation, and the flux of Pacific asthenosphere into the Caribbean realm. *Geology*, *29*(2), 127–130.

Allmendinger, R. W., Loveless, J. P., Pritchard, M. E., & Meade, B. (2009). From decades to epochs: Spanning the gap between geodesy and structural geology of active mountain belts. *Journal of Structural Geology*, *31*(11), 1409–1422.

Alvarado, G. E., & Gans, P. B. (2012). Síntesis geocronológica del magmatismo, metamorfismo y metalogenia de Costa Rica, América Central. *Revista Geológica de América Central*(46).

Argus, D. F., Gordon, R. G., & DeMets, C. (2011). Geologically current motion of 56 plates relative to the no-net-rotation reference frame. *Geochemistry, Geophysics, Geosystems*, *12*(11). doi: 10.1029/2011GC003751

Bangs, N. L., McIntosh, K. D., Silver, E. A., Kluesner, J. W., & Ranero, C. R. (2015). Fluid accumulation along the Costa Rica subduction thrust and development of the seismogenic zone. *Journal of Geophysical Research: Solid Earth*, *120*(1), 67–86. doi: 10.1002/2014JB011265

Bangs, N. L., McIntosh, K. D., Silver, E. A., Kluesner, J. W., & Ranero, C. R. (2016). A recent phase of accretion along the southern Costa Rican subduction zone. *Earth and Planetary Science Letters*, *443*, 204–215.

Barckhausen, U., Ranero, C. R., von Huene, R., Cande, S. C., & Roeser, H. A. (2001). Revised tectonic boundaries in the Cocos Plate off Costa Rica: Implications for the segmentation of the convergent margin and for plate tectonic models. *Journal of Geophysical Research*, *106*(B9), 19207–19220.

Brandes, C., Astorga, A., Back, S., Littke, R., & Winsemann, J. (2007). Deformation style and basin-fill architecture of the offshore Limón back-arc basin (Costa Rica). *Marine and Petroleum Geology*, *24*, 277–287. doi: 10.1016/j.marpetgeo.2007.03.002

Bronk Ramsey, C. (2009). Bayesian analysis of radiocarbon dates. *Radiocarbon*, *51*(1), 337–360.

Buchs, D., Baumgartner, P., Baumgartner-Mora, C., Bandini, A. N., Jackett, S.-J., Diserens, M.-O., & Stucki, J. (2009). Late Cretaceous to Miocene seamount accretion and mélange formation in the Osa and Burica Peninsula (Southern Costa Rica): episodic growth of a convergent margin. *Geological Society, London, Special Publications*, *328*, 411–456. doi: 10.1144/SP328.17

Buchs, D. M., Arculus, R. J., Baumgartner, P. O., Baumgartner-Mora, C., & Ulianov, A. (2010). Late Cretaceous arc development on the SW margin of the Caribbean Plate: Insights from the Golfito, Costa Rica, and Azuero, Panama, complexes. *Geochemistry, Geophysics, Geosystems*, *11*(7). doi: doi:10.1029/2009GC002901

Clift, P. D., Pecher, I., Kukowski, N., & Hampel, A. (2003). Tectonic erosion of the Peruvian forearc, Lima Basin, by subduction and Nazca Ridge collision. *Tectonics*, *22*(3).

Clift, P. D., & Vannucchi, P. (2004). Controls on tectonic accretion versus erosion

in subduction zones: Implications for the origin and recycling of the continental crust. *Review of Geophysics*, *42*, 1–31.

Corrigan, J., Mann, P., & Ingle, J. C. (1990). Forearc response to subduction of the Cocos Ridge, Panama-Costa Rica. *Geological Society of America Bulletin*, *102*, 628–652.

Cupper, M. L. (2006). Luminescence and radiocarbon chronologies of playa sedimentation in the Murray Basin, southeastern Australia. *Quaternary Science Reviews*, *25*(19-20), 2594–2607.

Davis, D., Suppe, J., & Dahlen, F. (1983). Mechanics of fold-and-thrust belts and accretionary wedges. *Journal of Geophysical Research: Solid Earth*, *88*(B2), 1153–1172.

de Boer, J. Z., Drummond, M. S., Bordelon, M. J., Defant, M. J., Bellon, H., & Maury, R. C. (1995). Cenozoic magmatic phases of the Costa Rican island arc (Cordillera de Talamanca). In P. Mann (Ed.), *Geologic and tectonic development of the caribbean plate boundary in southern central america* (pp. 35–55). Boulder, Colorado: Geological Society of America-Special Paper 295.

DeMets, C. (2001). A new estimate for present-day Cocos-Caribbean plate motion: Implications for slip along the Central American volcanic arc. *Geophysical Research Letters*, *28*(21), 4043–4046.

Denyer, P., Baumgartner, P., & Gazel, E. (2006). Characterization and tectonic implication of Mesozoic-Cenozoic oceanic assemblages of Costa Rica and Western Panama. *Geologica Acta*, *4*(102), 219–235.

Dominguez, S., Malavieille, J., & Lallemand, S. (2000). Deformation of accretionary wedges in response to seamount subduction: Insights from sandbox experiments. *Tectonics*, *19*(1), 182–196.

Dzierma, Y., Rabbel, W., Thorwart, M. M., Flueh, E. R., Mora, M. M., & Alvarado, G. E. (2011). The steeply subducting edge of the Cocos Ridge: Evidence from receiver functions beneath the northern Talamanca Range, south-central Costa Rica. *Geochemistry, Geophysics, Geosystems*, *12*(4). doi: 10.1029/2010GC003477

Edwards, J. H., Kluesner, J. W., Silver, E. A., & Bangs, N. L. (2018). Pleistocene vertical motions of the Costa Rican outer forearc from subducting topography and a migrating fracture zone triple junction. *Geosphere*, *14*(2), 510–534.

Fisher, D. M., Gardner, T. W., Marshall, J. S., & Monetero, P. W. (1994). Kinematics associated with late Cenozoic deformation in central Costa Rica: Western boundary of the Panama microplate. *Geology*(22), 263–266.

Fisher, D. M., Gardner, T. W., Marshall, J. S., Sak, P. B., & Protti, M. (1998). Effect of subducting seafloor roughness on fore-arc kinematics, Pacific coast, Costa Rica. *Geology*, *26*(6), 467–470.

Fisher, D. M., Gardner, T. W., Sak, P., Sanchez, J. D., Murphy, K., & Vannucchi, P. (2004). Active thrusting in the inner forearc of an erosive convergent margin, Pacific coast, Costa Rica. *Tectonics*, *23*. doi: 10.1029/2002TC001464

Galbraith, R., Roberts, R., Laslett, G., Yoshida, H., & Olley, J. (1999). Optical dating of single and multiple grains of quartz from Jinmium Rock Shelter, northern Australia: Part I: Experimental design and statistical models. *Archaeometry*, *41*, 339–364. doi: 10.1111/j.1475-4754.1999.tb00987.x

Gardner, T. W., Fisher, D. M., Morell, K. D., & Cupper, M. (2013). Upper-plate deformation in response to flat slab subduction inboard of the aseismic Cocos Ridge, Osa Peninsula, Costa Rica. *Lithosphere*, *5*(3), 247–264. doi: 10.1130/L251.1

Gardner, T. W., Verdnock, D., Pinter, N. M., Slingerland, R., Furlong, K. P., Bullard, T. F., & Wells, S. G. (1992). Quaternary uplift astride the aseismic Cocos Ridge, Pacific Coast, Costa Rica. *Geological Society of America Bulletin*, *29*(2), 219–232.

Gonzalez, V., Paul, R., Nichols, K., & Dylan, R. (2016). Long-term erosion rates of Panamanian drainage basins determined using in situ ^{10}Be. *Geomorphology*.

Gräfe, K., Frisch, W., Villa, I. M., & Meschede, M. (2002). Geodynamic evolution of southern Costa Rica related to low-angle subduction of the Cocos Ridge: constraints from thermochronology. *Tectonophysics*, *348*, 187–204.

Harris, R., Sakaguchi, A., Petronotis, K., Baxter, A., Berg, R., Burkett, A., ... others (2013). Expedition 344 summary. In *Proc. iodp— volume* (Vol. 344, p. 2).

Hayes, G. P., Wald, D. J., & Johnson, R. L. (2012). Slab1. 0: A three-dimensional model of global subduction zone geometries. *Journal of Geophysical Research: Solid Earth (1978–2012)*, *117*(B1). doi: 10.1029/2011JB008524

Hinz, K. (1996). Tectonic structure of the convergent Pacific margin offshore Costa Rica from multichannel seismic reflection data. *Tectonics*, *15*(1), 54.

Hoernle, K., van den Bogaard, P., Werner, R., Lissinna, B., Hauff, F., Alvarado, G., & Garbe-Schonberg, D. (2002). Missing history (16-71 Ma) of the Galápagos hotspot: Implications for the tectonic and biological evolution of the Americas. *Geology*, *30*(9), 795–798.

Kesel, R. H. (1983). Quaternary history of the Río General Valley, Costa Rica. *National Geographic Society Research Reports*, *15*, 339–358.

Kobayashi, D., LaFemina, P., Geirsson, H., Chichaco, E., Abrego, A. A., Mora, H., & Camacho, E. (2014). Kinematics of the western Caribbean: Collision of the Cocos Ridge and upper plate deformation. *Geochemistry, Geophysics, Geosystems*, *15*, 1671–683. doi: 10.1002/2014GC005234

Kolarsky, R. A., Mann, P., & Monetero, P. W. (1995). Island Arc Response to Shallow Subduction of the Cocos Ridge, Costa Rica. In P. Mann (Ed.), *Geologic and tectonic development of the caribbean plate boundary in southern central america* (pp. 235–262). Boulder, Colorado: Geological Society of America Special Paper 295.

Lambeck, K., & Chappell, J. (2001). Sea Level Change through the Last Glacial Cycle. *Science*, *292*(5517), 679–686.

Lambeck, K., Rouby, H., Purcell, A., Sun, Y., & Sambridge, M. (2014). Sea level and global ice volumes from the Last Glacial Maximum to the Holocene. *Proceedings of the National Academy of Sciences*, *111*(43), 15296–15303.

Laursen, J., Scholl, D. W., & Von Huene, R. (2002, September). Neotectonic deformation of the central Chile margin: Deepwater forearc basin formation in response to hot spot ridge and seamount subduction. *Tectonics*, *21*(5), 2–1–2–27. doi: 10.1029/2001TC901023

Lester, R., McIntosh, K., Van Avendonk, H. J., Lavier, L., Liu, C.-S., & Wang, T. (2013). Crustal accretion in the Manila trench accretionary wedge at the transition from subduction to mountain-building in Taiwan. *Earth and Planetary Science Letters*, *375*, 430–440.

Lonsdale, P., & Klitgord, K. D. (1978). Structure and tectonic history of the eastern Panama Basin. *Geological Society of America Bulletin*, *89*, 981–999.

MacKay, M. E., & Moore, G. F. (1990). Variation in deformation of the South Panama accretionary prism: response to oblique subduction and trench sediment variation. *Tectonics*, *9*(4), 683–698.

MacMillan, I., Gans, P. B., & Alvarado, G. (2004). Middle Miocene to present plate tectonic history of the southern Central American Volcanic Arc. *Tectonophysics*, *392*, 325–348. doi: 10.1016/j.tecto.2004.04.014

Marshall, J. S., & Anderson, R. S. (1995). Quaternary uplift and seismic cycle deformation, Peninsula de Nicoya, Costa Rica. *Bulletin of the Geological Society of America*, *107*(4), 463–473.

Marshall, J. S., Fisher, D. M., & Gardner, T. W. (2000). Central Costa Rica deformed belt: Kinematics of diffuse faulting across the western Panama Block. *Tectonics*, *19*(3), 468–492.

McIntosh, K., Silver, E., & Shipley, T. (1993). Evidence and mechanisms for forearc extension at the accretionary Costa Rica convergent margin. *Tectonics*, *12*(6),

1380–1392.

McKenzie, D. P., & Morgan, W. (1969). Evolution of triple junctions. *Nature*, *224*, 125–133.

Mescua, J. F., Porras, H., Durán, P., Giambiagi, L., de Moor, M., Cascante, M., ... Poblete, F. (2017). Middle to late Miocene contractional deformation in Costa Rica triggered by plate geodynamics. *Tectonics*, *36*(12), 2936–2949.

Moore, G. F., & Sender, K. L. (1995). Fracture zone collision along the south Panama margin. In P. Mann (Ed.), *Geologic and tectonic development of the caribbean plate boundary in southern central america. geological society of america special paper, 295* (pp. 201–212). Boulder, CO: Geological Society of America, Inc.

Morell, K. D. (2015). Late Miocene to recent plate tectonic history of the southern Central America convergent margin. *Geochemistry, Geophysics, Geosystems*, *16*(10), 3362–3382.

Morell, K. D. (2016). Seamount, ridge, and transform subduction in southern Central America. *Tectonics*, *35*(2), 357–385.

Morell, K. D., Fisher, D. M., & Gardner, T. W. (2008). Inner forearc response to subduction of the Panama Fracture Zone, southern Central America. *Earth and Planetary Science Letters*, *265*, 82–95. doi: 0.1016/j.epsl.2007.09.039

Morell, K. D., Fisher, D. M., Gardner, T. W., LaFemina, P. C., Davidson, D., & Teletzke, A. (2011). Quaternary outer fore-arc deformation and uplift inboard of the Panama Triple Junction, Burica Peninsula. *Journal of Geophysical Research*, *116*(B05402). doi: 10.1029/2010JB007979

Morell, K. D., Gardner, T. W., Fisher, D. M., Idleman, B. D., & Zellner, H. M. (2013). Active thrusting, landscape evolution, and late Pleistocene sector collapse of Barú Volcano above the Cocos-Nazca slab tear, southern Central America. *Geological Society of America Bulletin*, *125*(7-8), 1301–1318. doi: 10.1130/B30771.1

Morell, K. D., Kirby, E., Fisher, D. M., & van Soest, M. (2012). Geomorphic and exhumational response of the Central American Volcanic Arc to Cocos Ridge subduction. *Journal of Geophysical Research*, *117*(B04409). doi: 10.1029/2011JB008969

Murray, A., & Roberts, R. (1998). Measurement of the equivalent dose in quartz using a regenerative-dose single-aliquot protocol. *Radiation measurements*, *29*(5), 503–515.

Murray, A. S., & Wintle, A. G. (2000). Luminescence dating of quartz using an improved single-aliquot regenerative-dose protocol. *Radiation measurements*, *32*(1), 57–73.

Olley, J. M., Roberts, R. G., Yoshida, H., & Bowler, J. M. (2006). Single-grain optical dating of grave-infill associated with human burials at Lake Mungo, Australia. *Quaternary Science Reviews*, *25*, 2469–2474. doi: 10.1016/j.quascirev.2005.07.022

Ouimet, W. B., Whipple, K., & Granger, D. (2009). Beyond threshold hillslopes: Channel adjustment to base-level fall in tectonically active mountain ranges. *Geology*, *37*(9). doi: 10.1130/G30013A.1

Phillips, J. S. (1983). *Stratigraphy, sedimentology and petrologic evolution of Tertiary sediments in southern Costa Rica* (Unpublished master's thesis). Lousiana State University, Baton Rough, LA. (153 pp.)

Ranero, C. R., Grevemeyer, I., Sahling, H., Barckhausen, U., Hense, C., Wallmann, K., ... McIntosh, K. (2008). Hydrogeological system of erosional convergent margins and its influence on tectonics and interplate seismogenesis. *Geochemistry, Geophysics, Geosystems*, *9*(3). doi: 10.1029/2007GC001679

Ranero, C. R., Phipps Morgan, J., & Reicher, C. (2003). Bending-related faulting and mantle serpentinization at the Middle America Trench. *Nature*, *425*, 367–373. doi: 10.1038/nature01961

Ranero, C. R., & von Huene, R. (2000). Subduction erosion along the Middle America convergent margin. *Nature*, *404*, 748–752.

Reimer, P. J., Bard, E., Bayliss, A., Beck, J. W., Blackwell, P. G., Ramsey, C. B., ... others (2013). IntCal13 and Marine13 radiocarbon age calibration curves 0–50,000 years cal BP. *Radiocarbon*, *55*(4), 1869–1887.

Rooney, T. O., Morell, K. D., Hidalgo, P., & Fraceschi, P. (2015). Magmatic consequences of the transition from orthogonal to oblique subduction in Panama. *Geochemistry, Geophysics, Geosystems*, *16*(12), 4178–4208.

Sak, P. B., Fisher, D. M., & Gardner, T. W. (2004). Effects of subducting seafloor roughness on upper plate vertical tectonism: Osa Peninsula, Costa Rica. *Tectonics*, *23*(TC1017). doi: 10.1029/2002TC001474

Sak, P. B., Fisher, D. M., Gardner, T. W., Marshall, J. S., & La Femina, P. C. (2009). Rough crust subduction, forearc kinematics, and Quaternary uplift rates, Costa Rican segment of the Middle America Trench. *Geological Society of America Bulletin*, *121*(7/8), 992–1012. doi: 10.1130/B26237.1

Sallarès, V., Danobeitia, J. J., Flueh, E. R., & Leandro, G. (1999). Seismic velocity structure across the Middle American landbridge in northern Costa Rica. *Journal of Geodynamics*, *27*(3), 327–344.

Silver, E. A., Reed, D. L., Tagudin, J. E., & Heil, D. J. (1990). Implication of the north and south Panama Thrust Belts for the origin of the Panama Orocline. *Tectonics*, *9*(2), 261–281.

Sitchler, J. C., Fisher, D. M., Gardner, T. W., & Protti, M. (2007). Constraints on inner forearc deformation from balanced cross sections, Fila Costeña thrust belt, Costa Rica. *Tectonics*, *26*. doi: 10.1029/2006TC001949

Stavenhagen, A., Flueh, E., Ranero, C., McIntosh, K., Shipley, T., Leandro, G., ... Danobeitia, J. (1998). Seismic wide-angle investigations in Costa Rica: A crustal velocity model from the Pacific to the Caribbean coast. *Z. Geol. Palaontol*, *1*(3-6), 393–406.

Taylor, F. W., Mann, P., Bevis, M. G., Edwards, R. L., Cheng, H., Cutler, K. B., ... Recy, J. (2005). Rapid forearc uplift and subsidence caused by impinging bathymetric features: examples from the New Hebrides and Solomon arcs. *Tectonics*, *24*(6), 23. doi: 10.1029/2004TC001650

Vannucchi, P., Morgan, J. P., & Balestrieri, M. L. (2016). Subduction erosion, and the de-construction of continental crust: The Central America case and its global implications. *Gondwana Research*, *40*, 184–198.

Vannucchi, P., Morgan, J. P., Silver, E. A., & Kluesner, J. W. (2016). Origin and dynamics of depositionary subduction margins. *Geochemistry, Geophysics, Geosystems*, *17*(6), 1966–1974.

Vannucchi, P., Sak, P. B., Morgan, J. P., Ohkushi, K., & Ujiie, K. (2013, July). Rapid pulses of uplift, subsidence, and subduction erosion offshore Central America: Implications for building the rock record of convergent margins. *Geology*, *41*(9), 995–998. doi: 10.1130/G34355.1

Vannucchi, P., Scholl, D. W., Meschede, M., & McDougall-Ried, K. (2001). Tectonic erosion and consequent collapse of the Pacific margin of Costa Rica: Combined implications for ODP Leg 170, seismic offshore data, and regional geology of the Nicoya Peninsula. *Tectonics*, *20*(5), 649–668.

Vannucchi, P., Ujiie, K., Stroncik, N., Malinverno, A., Arroyo, I., Barckhausen, U., ... others (2011). Costa Rica Seismogenesis Project (CRISP): sampling and quantifying input to the seismogenic zone and fluid output.

von Huene, R., Bialas, J., Flueh, E., Cropp, B., Csernok, T., Fabel, E., ... Barrios L., O. (1995). Morphotectonics of the Pacific convergent margin of Costa Rica. In P. Mann (Ed.), *Geologic and tectonic development of the caribbean plate boundary in southern central america* (pp. 291–307). Boulder Colorado: Geological Society of America Special Paper 295.

von Huene, R., & Ranero, C. R. (2003). Subduction erosion and basal friction along the sediment-starved convergent margin off Antofagasta, Chile. *Journal of Geophysical Research*, *108*.

von Huene, R., Ranero, C. R., & Vannucchi, P. (2004). Generic model of subduction erosion. *Geology*, *32*(10), 913–916.

von Huene, R., Ranero, C. R., & Weinrebe, W. (2000). Quaternary convergent margin tectonics of Costa Rica, segmentation of the Cocos Plate, and Central American volcanism. *Tectonics*, *19*(19), 314–334.

von Huene, R., & Scholl, D. W. (1991). Observations at convergent margins concerning sediment subduction, subduction erosion, and the growth of continental crust. *Review of Geophysics*, *29*, 279–316.

Walther, C. H. E. (2003). The crustal structure of the Cocos ridge off Costa Rica. *Journal of Geophysical Research*, *108*(B3). doi: 10.1029/2001JB000888

Wegner, W., Wörner, G., Harmon, R., & Jicha, B. R. (2010). Magmatic history and evolution of the Central American Land Bridge in Panama since Cretaceous times. *Geological Society of America Bulletin*, *123*(3-4), 703–724. doi: 10.1130/B30109.1

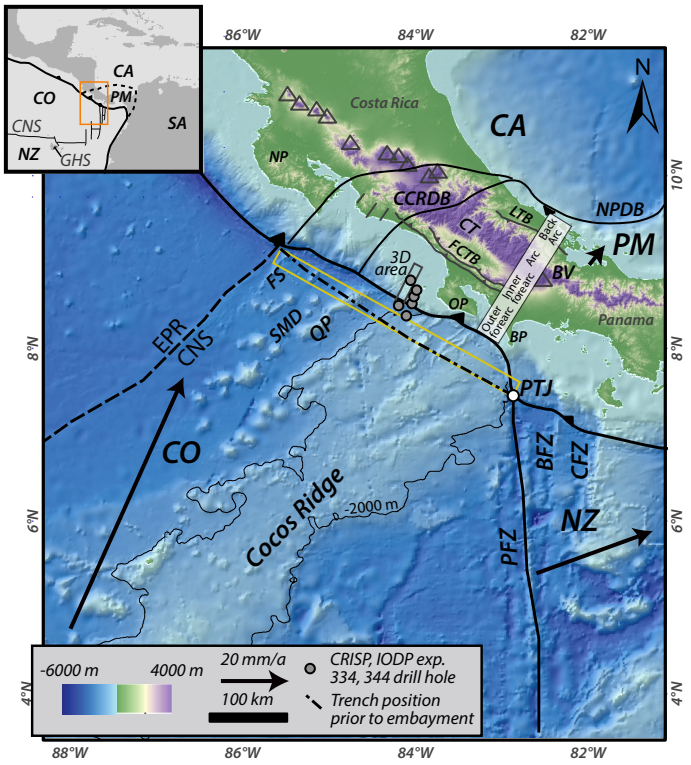

Figure 1. Regional tectonic setting of the southern Costa Rica subduction zone. Costa Rica Seismogenesis Project (CRISP) 3D seismic area denoted by '3D area' box. Black arrows show plate motion relative to stable Caribbean plate (CA) (DeMets, 2001; Argus et al., 2011; Kobayashi et al., 2014). Dot-dashed line shows former position of the trench following Vannucchi et al. (2013). Yellow box shows bathymetry swath and location of crustal thickness data from Walther (2003) as shown in Figure 7. Triangles show currently-active volcanoes. Large-scale tectonic features compiled from Silver et al. (1990), Kolarsky et al. (1995), Fisher et al. (1998), Marshall et al. (2000), Barckhausen et al. (2001), Fisher et al. (2004), Sitchler et al. (2007), and Brandes et al. (2007). BFZ, Balboa Fracture Zone; BP, Burica Peninsula; BV, Barú Volcano; CA, Caribbean plate; CCRDB, Central Costa Rica Deformed Belt; CNS, Cocos-Nazca Spreading Center; CO, Cocos plate; CFZ, Coiba Fracture Zone; CT, Cordillera de Talamanca; EPR, East Pacific Rise; FCTB, Fila Costeña Thrust Belt; FS, Fisher Seamount; GHS, Galápagos Hot Spot; LTB, Limón Thrust Belt; NP, Nicoya Peninsula; NPDB, North Panama Deformed Belt; NZ, Nazca Plate; OP, Osa Peninsula; PM, Panama microplate; PTJ, Panama Triple Junction; QP, Quepos Plateau; SA, South America Plate; SMD, Seamount domain. Bathymetry from GEBCO (General Bathymetric Chart of the Oceans) and Ranero et al. (2003). Topography from NASA's Shuttle Radar Topography Mission (SRTM) 90-m dataset and GTOPO-30.

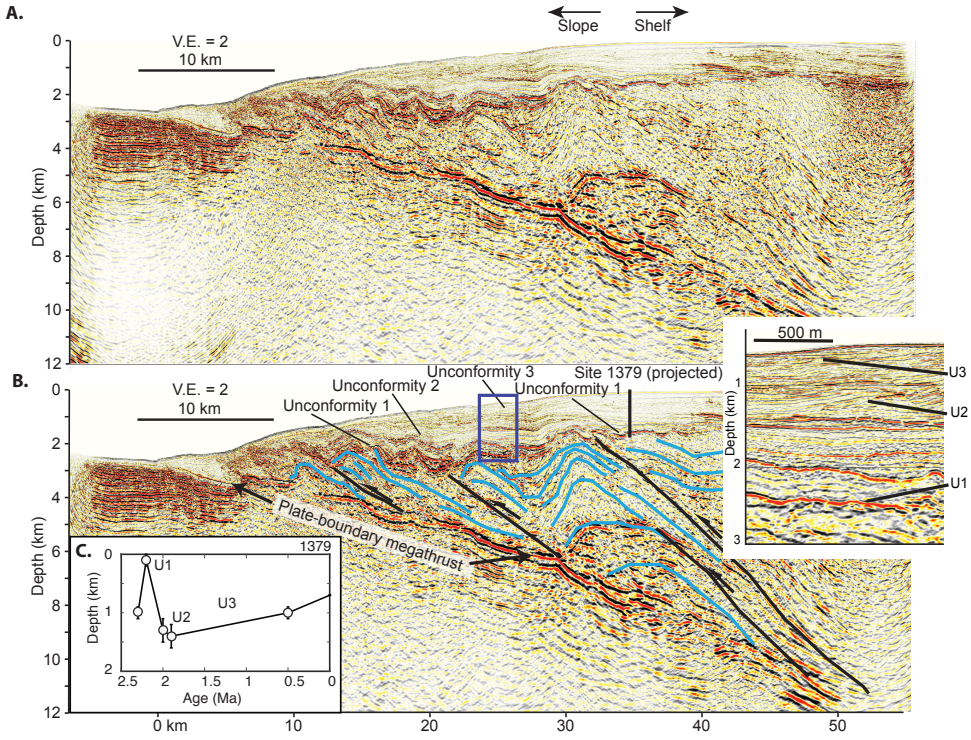

Figure 2. **A.** Uninterpreted seismic section from the Costa Rica Seismogenesis Project (CRISP) 3D volume, with location shown in Figure 1. V.E. denotes vertical exaggeration. **B.** Interpreted section as in A showing location of unconformities, faults and folds (Bangs et al., 2016; Edwards et al., 2018). Dark blue box shows location of blow-up. **C.** Uplift or subsidence data from core at site 1379 after backstripping for the effects of sediment loading from Vannucchi et al. (2013). U1, U2 and U3 refer to unconformities 1, 2 and 3, respectively.

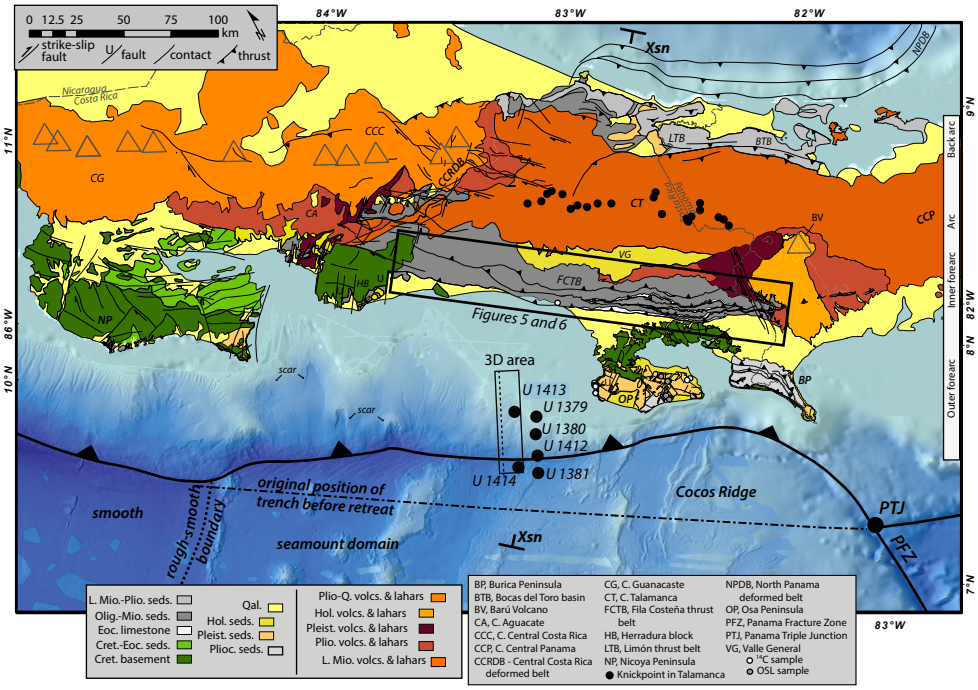

Figure 3. Geologic map of Costa Rica and western Panama modified from Morell (2016) and references therein. Bathymetric data and bathymetric scale same as Figure 1. Triangles denote active volcanoes. U refers to upthrown tectonic block. Locations of radiocarbon (^{14}C) and OSL samples from Gardner et al. (1992) Fisher et al. (2004), Sak et al. (2004), Sak et al. (2009), and Gardner et al. (2013). See Tables 2 and 3 for more information about samples. Knickpoint locations from Morell et al. (2012). Xsn refers to cross section location in Figure 4. Dashed line in 3D area shows location of Figure 2.

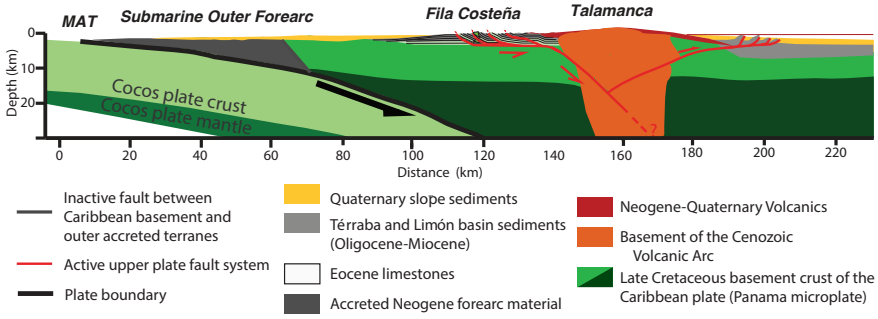

Figure 4. Cross section of the Costa Rican forearc-arc-backarc system along transect in Figure 3 (labelled as 'xsxn') based on Stavenhagen et al. (1998), Hayes et al. (2012), D. Buchs et al. (2009), Fisher et al. (2004), Brandes et al. (2007), and Morell et al. (2012).

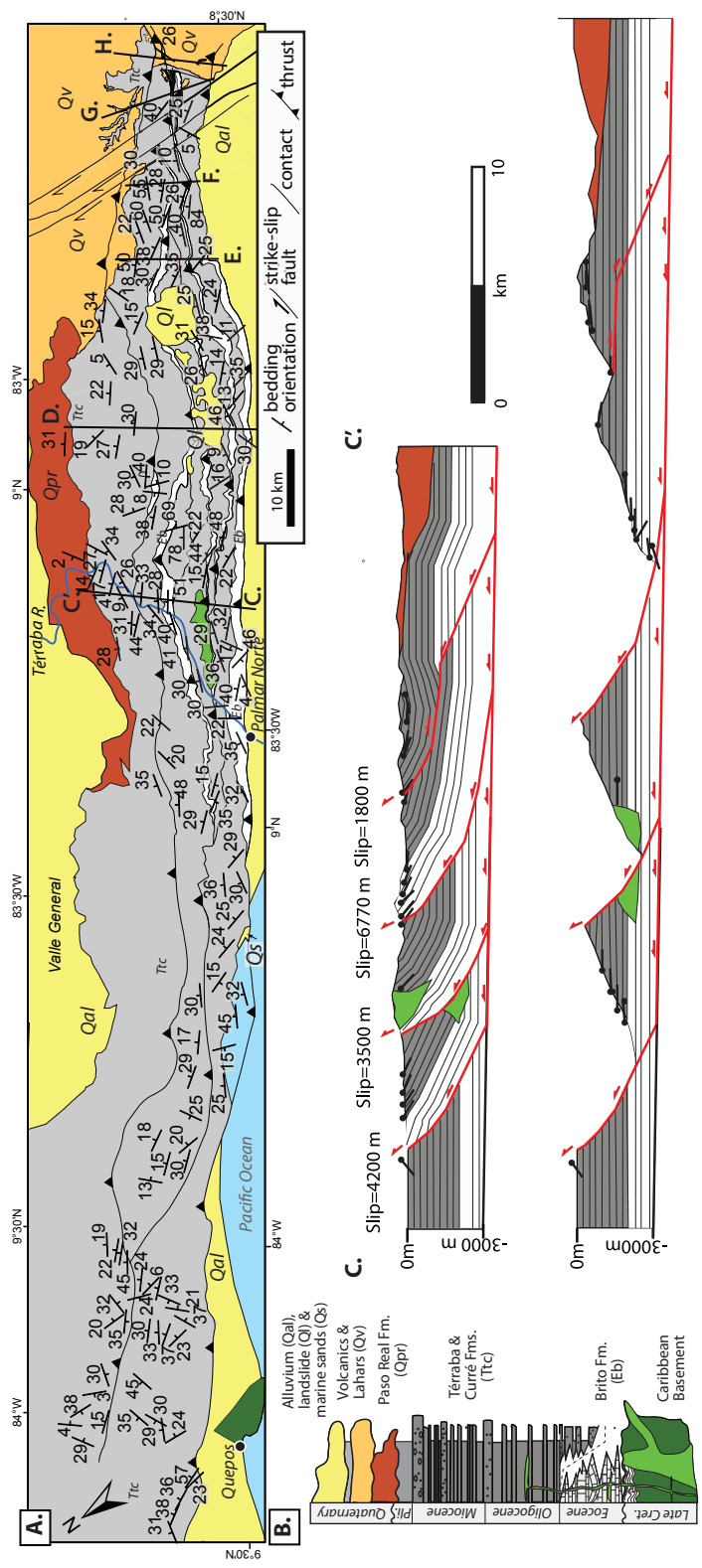

Figure 5. **A.** Geologic map of the Fila Costeña Thrust Belt, showing ~75 new bedding orientation data combined with previously published data from Fisher et al. (2004), Sitchler et al. (2007), Morell et al. (2008), Sak et al. (2009), Morell et al. (2013), and Morell (2016). The décollement beneath the Fila Costeña steps up-section in the northwestern portion of the thrust belt, and therefore does not expose the Brito Fm. Thrust locations in this northwestern region are therefore mapped based on field observations of fault contacts, and projected along strike parallel to the topographic grain. **B.** Stratigraphic column of the Central Fila Costeña Thrust Belt showing units displayed in part A, modified from Phillips (1983) and Fisher et al. (2004). **C.** New balanced cross section based on data following the Térraba River (see location in part A). Cross section constructed by forward modeling to match mapped contacts, thrust traces and surface structural measurements in 2D Move. The cross-section was constructed taking into account both the dip measurements shown, as well as data from the regional mapped structure, which suggests that thrust faults do not change orientation significantly along strike and on average dip consistently to the northeast by 15-35°.

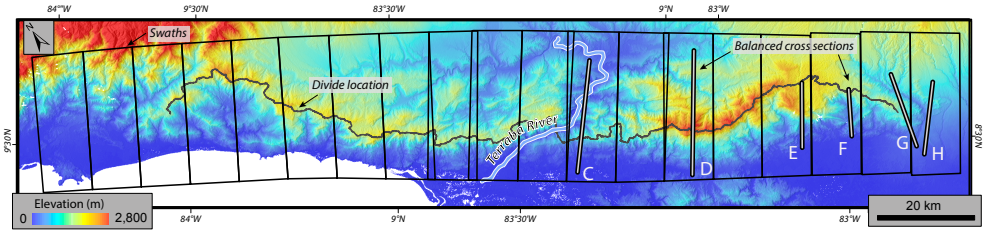

Figure 6. Digital elevation model and topography of the Fila Costeña Thrust Belt, showing swath locations used in cross-sectional area calculations. Map extent shown in Figure 3 and is the same as Figure 5. Topography from NASA's SRTM 30-m dataset. Black line shows topographic divide shown in Figure 7A. Mean and 1σ cross-sectional areas calculated within each swath are reported in Figure 7B. Line-length balanced cross section locations are shown as in Figure 5, from Fisher et al. (2004), Sitchler et al. (2007), Morell et al. (2008), Morell et al. (2013) and this study.

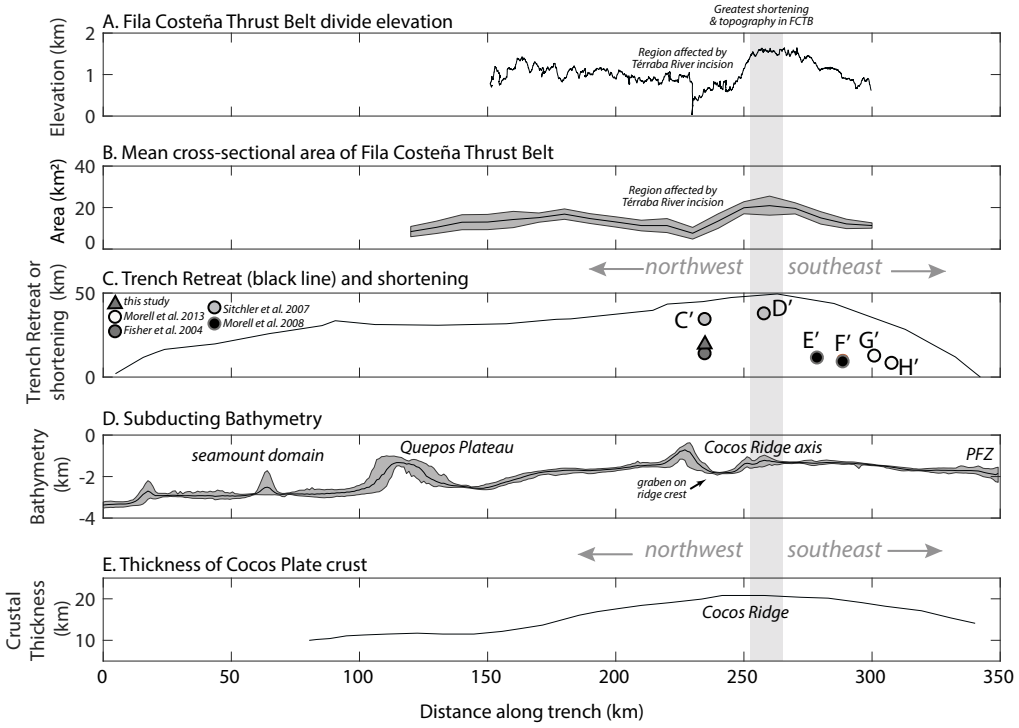

Figure 7. **A.** Elevation of the Fila Costeña Thrust Belt (FCTB) drainage divide from data in Figure 6. **B.** Mean cross-sectional area of Fila Costeña Thrust Belt relative to current sea level and 1σ uncertainty within 10 km wide and 30 km long swaths as shown in Figure 6. Topographic analysis based on SRTM-30-m data. **C.** Trench retreat estimated following Vannucchi et al. (2013) as the distance between the present-day trench and the assumed projection shown as dot-dashed line in Figures 1 and 3. Shortening estimates across the Fila Costeña from cross-sections as shown in Figure 5 (denoted as C'-H') are derived from this study, Fisher et al. (2004), Sitchler et al. (2007), Morell et al. (2008), and Morell et al. (2013). Total shortening amounts along cross-sections E' and F' from Morell et al. (2008) are somewhat lower than adjacent cross-sections because they do not include slip along the rearmost thrust due to insufficient structural data in this region. **D.** Mean, maximum and minimum bathymetry along swath shown in Figure 1 from Ranero et al. (2003) relative to mean sea level. PFZ denotes Panama Fracture Zone. **E.** Thickness of Cocos plate crust on incoming plate along profile line shown in Figure 1 (Sallarès et al., 1999; Walther, 2003).

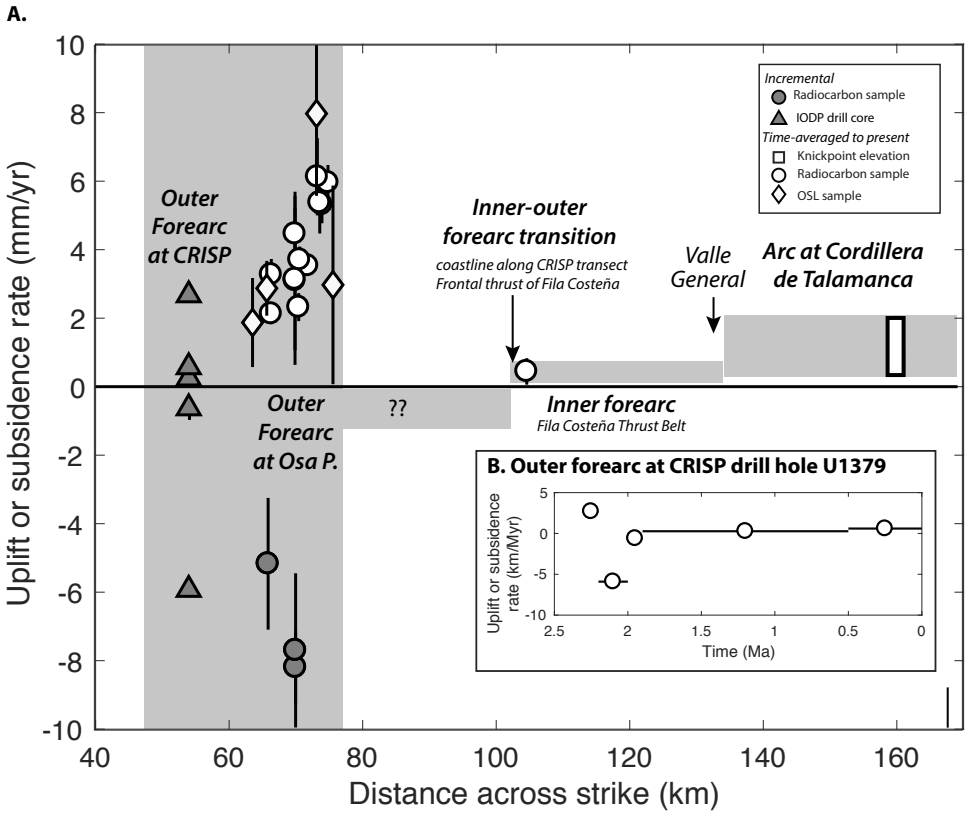

Figure 8. **A.** Rock uplift (positive) or subsidence (negative) rates compiled from offshore and onshore regions near the CRISP transect. See Figure 3 for location of samples. Offshore data derived from paleodepth calculations and backstripping from ocean drilling at hole U1379 (Vannucchi et al., 2011), with age control from nanofossil analysis and benthic foraminifera distribution (Table 1) (Vannucchi et al., 2013). Onshore data calculated from the elevation and ages of radiocarbon and OSL samples shown in Tables 2 and 3 with data from Gardner et al. (1992), Sak et al. (2004), Fisher et al. (2004), and Gardner et al. (2013). Ranges of rock uplift rates are reported for the Talamanca Range calculated from the elevation of 21 knickpoints relative to current base level, and an onset of increased rock uplift starting at 1, 2 or 3 Ma (Morell et al., 2012). **B.** Calculated incremental uplift or subsidence rates based on data from Vannucchi et al. (2013) and Vannucchi, Morgan, Silver, & Kluesner (2016) from data shown in Table 1.

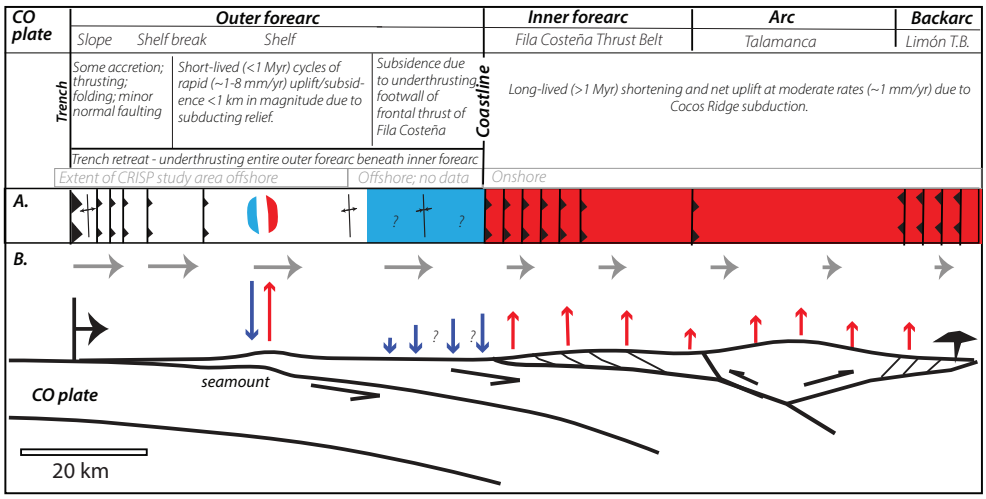

Figure 9. Cartoon showing proposed model for the Quaternary evolution of the outer forearc of southern Costa Rica along the CRISP transect. Panel A shows map-view cartoon depiction of uplift (red) or subsidence (blue) along the transect. Panel B shows locations of relative rates of uplift (red arrows) or subsidence (blue arrows) at positions along the transect. Grey arrows show relative movement of the forearc towards a pinned back arc. Vertical scale is exaggerated to highlight important features and is not to scale. The coastline demarcates a dichotomy in vertical tectonics between the offshore forearc and the inner forearc-arc-backarc system. The submarine forearc records: 1) yo-yo tectonics and sharp reversals between periods of rapid subsidence and uplift that last less than ∼1 Myr (Vannucchi et al., 2013; Vannucchi, Morgan, Silver, & Kluesner, 2016) as a consequence of subducting bathymetric relief, similar to results from the Osa Peninsula (Sak et al., 2004; Gardner et al., 2013). The onland inner forearc-arc-backarc system records: 1) telescoping of the forearc (Fisher et al., 2004; Sitchler et al., 2007; Morell et al., 2008, 2013) and backarc (Silver et al., 1990; Brandes et al., 2007) basins; and 2) long term uplift across the inner forearc at the Fila Costeña (Fisher et al., 1998, 2004; Sak et al., 2009), volcanic arc at the Cordillera de Talamanca (Morell et al., 2012), and the back arc at the Limón backarc thrust belt (Limón T.B.) (Brandes et al., 2007) due to Cocos Ridge subduction. CO indicates Cocos plate.